



ISSN (PRINT) : 2320 -1967  
ISSN (ONLINE) : 2320 -1975



## ORIGINAL ARTICLE

CHEMXPRESS 9(1), 080-090, (2016)

# Photocatalytic degradation of pathogenic bacteria using functionalized different sized ZnO nano films with 1-[(E)-1,3-benzothiazol-2-yl diazenyl]naphthalen-2-ol

H.R.Ravi<sup>1</sup>, P.N.Prashanth kumar<sup>2</sup>, H.R.Sreepad<sup>3</sup>

<sup>1</sup>Research centre, PG Department of physics, BETAHE, Bharthinagara, Mandya, (INDIA)

<sup>2</sup>Department of Industrial Chemistry, Kuvempu University, Shankaraghatta-577 451, (INDIA)

<sup>3</sup>Research centre, PG Department of physics, GFG College, Mandya, (INDIA)

E-mail: ravivr1@yahoo.in

Received : 16<sup>th</sup> January, 2015 ; Revised : 28<sup>th</sup> May, 2015 ; Accepted : 05<sup>th</sup> June, 2015

**Abstract :** This paper presents the high bacterial interaction strategy to improve the antimicrobial activity of visible-light-activated ZnO films. The manufacturing nanostructured semiconductor layers on the glass substrates prepared from the surfactant-assisted complex sol-gel method obtained different grain sized Zinc Oxide (ZnO) nanoparticles using zinc nitrate and citric acid as starting material. The effect of the citric acid concentration, varying the pH of the sol solution and PEG 2000 surfactant which affects the grain size of the ZnO nanoparticles. It was investigated using X-ray diffraction and UV-Visible absorbance spectroscopy. In this study, we demonstrated that functionalized Zinc oxide substrates having superior visible-light-induced bactericidal activity against Escherichia coli compared to pure Zinc oxide films. Particularly at pH=1 ZnO nano films surface complexed by benzothiophine dyes shifts the

wavelength towards higher region than the other pH values (3,5,7) which is mainly due to the smaller the grain size and rich in surface active sites which affects the adsorption of dyes. For obtaining the high photocatalytic performance is attributed to an effect of following factors: rich in active surface area of the ZnO films, an increase in absorption and shifting the wavelength towards visible region of the functionalized semiconducting films, From these findings suggest that ZnO functionalized films has potential applications in the development of alternative disinfections for environmental usages.

© Global Scientific Inc.

**Keywords :** ZnO nanocrystalline films; Benzothiazol sensitizer; Photocatalytic degradation of E- Coli bacteria.

## INTRODUCTION

Semiconductor-mediated photocatalytic oxida-

tion is regarded as a promising method for environmental decontamination. Among the semiconductors employed, ZnO is considered as a good photocata-

lyst because of its high photosensitivity, non-toxicity, easy availability, strong oxidizing power and long-term stability<sup>[1, 2]</sup>. Recently, there is a growing interest in photo-catalyst based on dye-sensitized semiconductor films<sup>[3]</sup>. In most cases the low cost materials and high demand for renewable energy sources have increased the use of dye sensitized solar cells. Numerous efforts have been done by several research groups all over the world to utilize natural dyes as sensitizers in dye-sensitized solar cells. A photo electrochemical cell utilizing flavonoid and anthocyanin dyes extracted from blackberries along with colloidal TiO<sub>2</sub> powder, was reported to convert sunlight to electrical power at an efficiency of 0.56% under full sun light<sup>[4]</sup>.

Heterostructures are formed by quantum-sized ZnO nanocrystals and photosynthetic pigments were prepared by adsorbing either chlorophyll, carotenoids or their mixture onto a film of organic-capped ZnO nanoparticles and were studied in the photo electrochemical processes. The photo conversion process was found to be greatly enhanced at the nanocrystalline electrodes upon sensitization with a dye mixture<sup>[5]</sup>. Chlorophyll derivatives and related natural porphyrins were used in photosensitization of titania solar cells<sup>[6]</sup>. Zinc oxide semiconductor was coated with extracts of natural pigments, chlorophyll or anthocyanin and used for the photo bleaching of rose bengal dye<sup>[7]</sup>. Sensitized TiO<sub>2</sub> was used in water purification in order to photodegraded organic pollutants such as Methyl Orange and Phenazpyridine<sup>[8]</sup>. Since Fujishima and Honda<sup>[9]</sup> reported the photocatalytic properties of TiO<sub>2</sub> in 1972, semiconductor photocatalysis has received a lot of attention<sup>[10, 11]</sup>. For instance, *Lactobacillus acidophilus*, *Saccharomyces cerevisiae*, and *Escherichia coli* were completely sterilized when incubated with platinum-loaded TiO<sub>2</sub> under metal halide lamp irradiation for 60–120 mins<sup>[12, 13]</sup>. TiO<sub>2</sub> photocatalysis is known to generate various active oxygen species, such as hydroxyl radicals, hydrogen peroxide, superoxide radical anions, etc., by redox reactions under UV irradiation whereas ZnO also generates active oxygen species<sup>[14]</sup>, which was responsible for inhibition of bactericidal growth. Such films, having large band gap semiconductors have been in-

vestigated, which themselves absorb only in the lower wavelength UV region. The ZnO photocatalyst is effective only upon irradiation by UV light at levels that would induce serious damage to human cells. This greatly restricts the potential applications of ZnO substrates for use in our living environments. Although solar energy is inexhaustible, only a few percent of its energy are in the UV range. ZnO cannot be an effective bactericidal medium unless there is sufficient irradiation time under bright sunlight. For offering the potential to overcome this problem an alternative method is necessary to enabling efficient harvesting of visible light. For harvesting the dyes that should be selected to get desired broad, strong absorption over the visible and near-infrared wavelength range. Hence, surface functionalization of metal oxide wide band gap semiconductor surfaces by covalently attaching transition-metal complexes or organic sensitizers are central in applications for degradation of organic compounds, solar energy conversion by dye-sensitized solar cells and degradation of micro organisms<sup>[13-19]</sup>.

However, most dyes are photochemically unstable and may not be able to absorb light in the desired wavelength range. Since 99% of the energy output from the sun is in the visible range, it is desirable for photosensitizers for sunlight-mediated disinfection to absorb visible light. For medical applications, absorbance in the near-infrared range is desirable, as these wavelengths penetrate more deeply into tissues than visible light. To adsorb these sensitizers it requires sufficient surface area of nanocrystalline ZnO films. Hence this chapter presents various sized ZnO nanoparticles was prepared by surfactant-assisted complex sol-gel method. The controlled preparation of zinc oxide (ZnO) nanoparticles using zinc nitrate and citric acid as starting material. ZnO nanoparticles with a pure wurtzite structure were obtained after calcination at 773 K. The effects of varying the pH of the sol solution, the optimized citric acid concentration, and the PEG-2000 surfactant controlled the average particle size of the ZnO nanoparticles was investigated by X-ray diffraction and UV-Visible spectrophotometer. The obtained various sized ZnO nanoparticles were coated on soda-lime glass substrate by previous tech-

# ORIGINAL ARTICLE

nique. i.e. doctor blade method. For investigation the performances of photocatalytic inactivation achieved by smaller grain sized ZnO film is better than that larger grain sized ZnO nanocrystalline coated samples, which as a result it because smaller grain size that was directly proportional to larger surface area, as a result it offers higher chemisorbtion of dyes over monolayer ZnO films.

The principle of functionalised ZnO photosensitization is illustrated in Scheme 1, which indicates the primary electron pathway<sup>[20]</sup>. When a dye molecule absorbs visible light, it is excited to a higher energy state. The excited dye\* then injects an electron to the conduction band of ZnO. The injected electron is scavenged by the surface-adsorbed O<sub>2</sub> to yield O<sub>2</sub><sup>•-</sup> and subsequently the OH radicals are responsible for bacterial inhibition growth. To the best of our knowledge Sondos Othman Abed-Alhadi Ateeq. et.al.<sup>[21]</sup> as recently, reported the investigation of anthocyanin sensitized ZnO catalyst in water containing E.coli bacteria. Hence, this chapter introduces a novel class of reported benzothioephine sensitizers anchoring on ZnO nanocrystalline films, which was used for analyzing the bactericidal activities, It was found that the films can kill E.coli (ATCC 25922) bacteria under visible light irradiation ( $\lambda > 420$  nm), effectively. Therefore we found that the higher photocatalytic inactivation achieved with pH =1 of ZnO coated film was better than that of other pH levels of ZnO-coated functionalized samples.

## EXPERIMENTAL

### Materials

Zn(NO<sub>3</sub>)<sub>2</sub>·6H<sub>2</sub>O, PEG-2000 surfactant, Aniline, potassium thiocyanate, glacial acetic acid was used

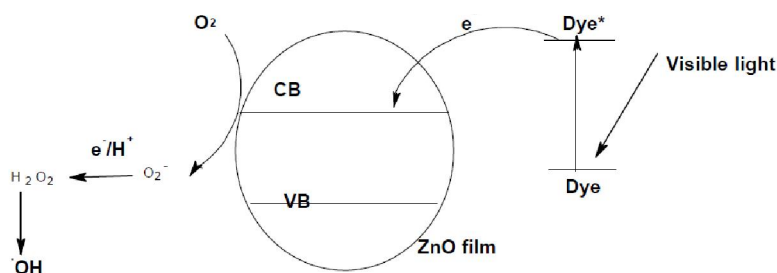
as starting materials, diazo liquor was freshly prepared using sodium nitrate and concentrated sulfuric acid. All the chemicals were purchased from Himedia laboratory and the reagents are analytical grade, and no needed for further purification.

### Spectral measurements

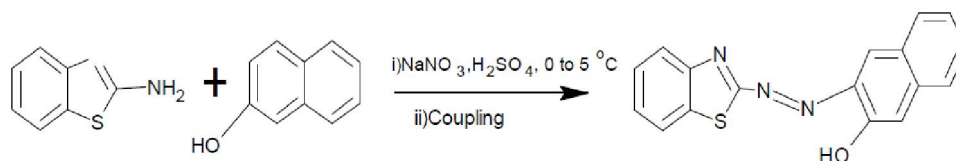
The <sup>1</sup>H NMR spectra were recorded on a Varian Gemini 300 (MHz) spectrometer; Mass spectra were recorded on LCMS-2010A SHIMADZU, UV-Visible spectrophotometer Shimadzu was used for optical absorbance measurements (UV-1650 model), IR spectra (nominal 4-cm<sup>-1</sup> resolution) were measured using a Digilab FTS-40 spectrometer, the dye powders were held in KBr pellets in case of N<sub>1</sub> sensitizers and the chemisorbed sensitizers on semiconducting oxide films were measured by attenuated total reflectance Infra red (ATR-IR) spectroscopy.

### Synthesis of 2 amino benzothiazol

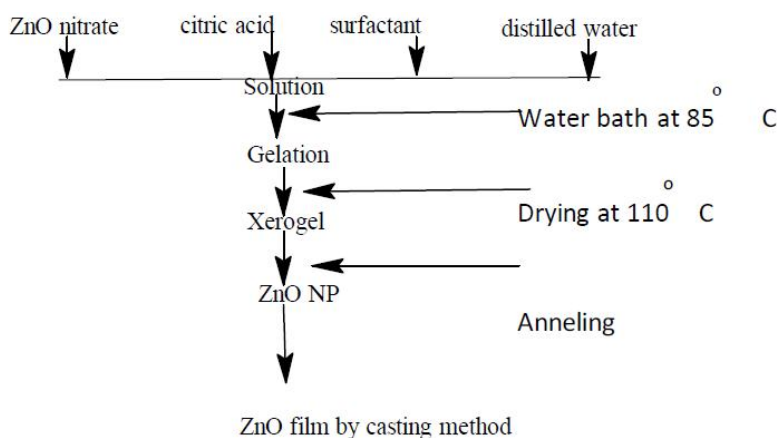
A mixture of aniline (0.01 M) and potassium thiocyanate (0.01 M) in glacial acetic acid (20 ml) was cooled and stirred in round bottom flask. To this solution bromine (0.01 M) was added by dropping funnel at such a rate that the temperature does not rise beyond 0°C. Then the bromine has been added to the above the solution was stirred for about 2hrs at 0°C. It was allowed to stand for overnight with an orange precipitate was settled at the bottom. To the precipitate water (6 ml) was added quickly slurry was heated at 85°C on steam bath and filtered under hot condition. The orange residue was placed in a reaction flask and treated with 10 ml of glacial acetic acid, heated again to 85°C and filtered in hot. The filtrate was cooled and neutralized with concentrated ammonia solution to pH 6 when dark yellow precipitate was appeared and recrystallized from benzene to obtain the 2 amino-benzothiazole.



Scheme 1



Scheme 2



Scheme 3

The completion of the reaction was monitored on TLC by using silica gel-G coated plates by using ethyl acetate and petroleum ether (7:3) as the eluent and the Mp ( $^\circ\text{C}$ ) = 125-127 $^\circ\text{C}$ .

### Preparation of 3-[1,3-benzothiazol-2-ylidiazenyl]naphthalen-2-ol [N1]

2-Aminobenzothiazole (2.0 mmol) was dissolved in the ratio of glacial acetic acid: propionic acid mixture (2:1, 6.0 ml) was quickly cooled in an ice/salt bath to 0-5  $^\circ\text{C}$ . A cold solution of nitrosylsulphuric acid (prepared from sodium nitrite (2.2 mmol,) and concentrated sulphuric acid (3 ml at 50 $^\circ\text{C}$ ) was added to the above solution and the mixture was stirred for an additional 3 hrs at the same temperature. Excess nitrous acid was destroyed by the addition of urea. Coupling compound (2.2 mmol) was wetted with Tween-80 (1% solution, few drops)<sup>[22]</sup>. To the above mixture, hot water (25 ml) and sodium hydroxide solution (7 ml, 10% w/v) was added slowly and the mixture was heated until a clear solution was appeared. The solution was cooled to 0-5  $^\circ\text{C}$  in an ice bath. Freshly prepared diazo liquor was added dropwise to this solution for over a period of an hour keeping the temperature of 0-5 $^\circ\text{C}$ . The reaction mixture was further stirred for 2 hrs at 0-5 $^\circ\text{C}$  and the pH was maintained 8.0 by adding the required amount of sodium

carbonate solution (10 % w/v). The product was filtered and washed several times with hot water to produce a dark red solid<sup>[23]</sup>. The solid was dissolved in DMF and precipitated by adding chloroform to produced final product. Yield 80%, obtained Mp ( $^\circ\text{C}$ ) = 208-210 (In literature 210-212; IR [(KBr) max/cm<sup>-1</sup>]: 1450.19cm<sup>-1</sup>(-N=N-), 1608cm<sup>-1</sup> (C=N); <sup>1</sup>H NMR (400 MHz, DMSO-d<sub>6</sub>): 15.47 (s, 1H, OH), 8.4(d 1H Ar H), 8.2 (t 2H Ar H), 7.8 (d 1H Ar H), 7.75(m, 1H Ar H), 7.6 (t, 1H, Ar H), 7.5(m, 2H, Ar H), 7.4 (t, 1H, Ar H), 6.8(d, 1H, Ar H).

### Preparation of ZnO nanoparticles

The uniform sized ZnO nanoparticles were prepared as followed in the reported literature procedure<sup>[24]</sup>. i.e. by adding the optimized concentration of (Czn+2/Ccit=1:1.5), PEG 2000 surfactant and the pH of the was solution was adjusted between 1 to 7 using NH<sub>3</sub>.H<sub>2</sub>O. The obtained ZnO nanoparticles containing organic and inorganic impurities was removed upon calcinations.

### Preparation of ZnO films

The prepared non-agglomerated different sized ZnO nanoparticles were ground in a porcelain mortar with a small amount of water (0.5ml) containing acetyl acetone to prevent re-aggregation of the particles. After the particles had been dispersed by the

# ORIGINAL ARTICLE

high shear forces in the paste, it was diluted by slow addition of water (1.5ml) under continuous grinding. Finally a surfactant (Triton X-100, Aldrich) was added to facilitate the spreading of the colloid on the substrate and then the paste was spread uniformly using a smooth glass stick with the draw rate around 2 cm/s. The thickness of the ZnO film was controlled by adhesive tape (thickness  $\sim 5\mu\text{m}$ ) surrounding the square film area. The films were heated at  $450^\circ\text{C}$  for 1h to decompose the organic paste between ZnO particles.

## Growth of the organism

Liquid cultures of *E. coli* (*Escherichia coli* ATCC 25922) were grown aerobically in Luria Broth (LB) at  $37^\circ\text{C}$  on a rotary shaker (170 rpm) for 18 hrs. The cells were centrifuged at 6000 rpm at  $4^\circ\text{C}$  for 5 min and suspended in 5 ml phosphate buffer solutions (PBS).

## Light source

A 100W tungsten halogen lamp was used. The irradiation light was filtered with a filter that cut off the light with wavelength below 420 nm. The intensity of the illumination was  $10\text{ mWcm}^{-2}$  on the catalyst surface during the experiment.

## Irradiation and experimental procedures

The cell suspension was diluted 105 times and then 2 ml of the diluted cell suspension was pipette

onto the coated ZnO films. For each sample,  $20\ \mu\text{l}$  cell solution was extracted by a pipette and spread on to the petri-dish containing LB culture medium followed by incubation for 24 h at  $37^\circ\text{C}$  and then finally the number of colonies on the dishes were counted.

## RESULT AND DISCUSSION

### XRD studies

The X-ray diffraction data were recorded by using Cu K $\alpha$  radiation (0.15406 nm). The intensity data were collected over a  $2\theta$  range of  $20\text{--}60^\circ$ . The average grain size of the samples was estimated with the help of Scherer equation using  $D = K\lambda / \beta \cos\theta$ , here K is constant,  $\lambda$  is the wavelength of X-ray radiation employed ( $1.54056\ \text{\AA}$ ),  $\beta$  is corrected full width at half maximum and  $\theta$  is Bragg angle. From the Figure 1A. shows that the XRD patterns of ZnO nanoparticles were corresponding to hexagonal wurtzite structure and all the diffraction peaks were in good agreement with the reported JCPDS card no. 89-139. No other characteristic peaks were observed other than ZnO nanoparticles and the obtained average crystallite size was about 10-50 nm. Experimental work reports that by varying the pH and citric acid concentration affects the grain size of the ZnO nanoparticles. Y.L.Zhang, et.al reported that low aggregative ZnO nanoparticles were obtained at the

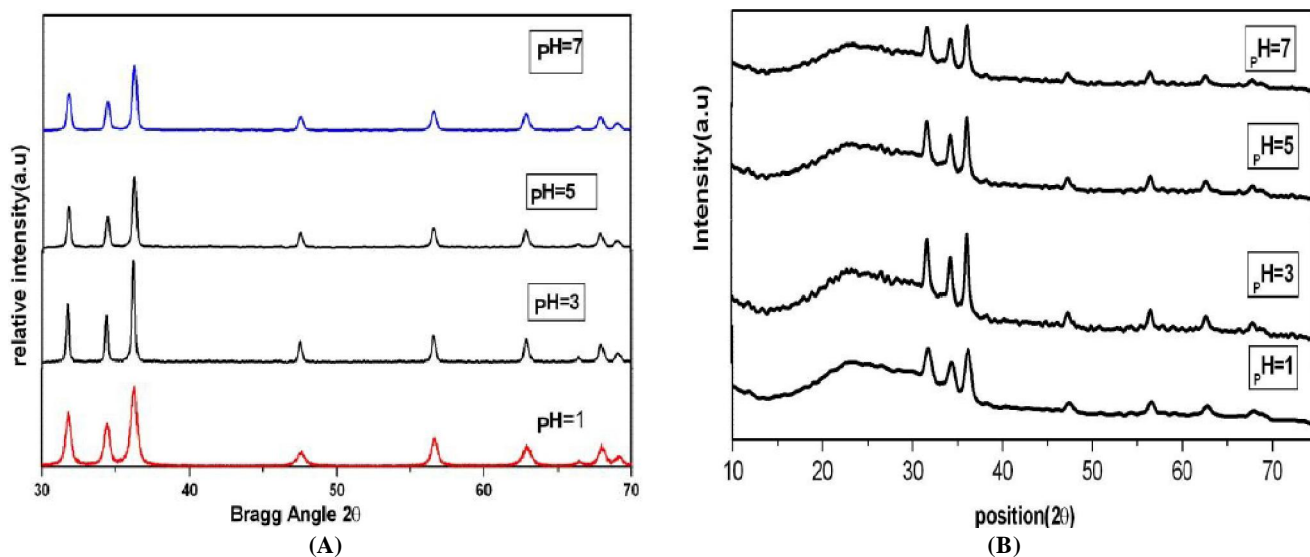


Figure 1 : XRD spectra's of different grain sized (A) ZnO nanoparticles and (B) ZnO nanocrystalline films (a) pH =1 (b) pH =3 (c) pH =5 and (d) pH =7

TABLE 1

PH	Conc. citric acid	Average grain size(nm) ZnO particles	Surface area by BET
pH=1	1:1.5	10	75
pH =3	1:1.5	48	16
pH =5	1:1.5	34	21.4
pH =7	1:1.5	29	26.78

TABLE 2

pH values	Conc. citric acid	Average grain size(nm)
pH =1	1:1.5	15
pH =3	1:1.5	53
pH =5	1:1.5	39
pH =7	1:1.5	32

optimized citric acid concentration is in the ratio of  $C_{Zn^{2+}}/C_{cit} = 1:1.5^{[24]}$ .

In our experiments, the effects of pH on the average grain size of the ZnO nanoparticles were estimated from XRD peaks as shown in Figure 1A. It was observed that grain size of the ZnO particles were minimal and the surface area was maximal at a pH 1. This was because the citric acid was incompletely ionized without  $NH_3 \cdot H_2O$  and acted as a bridge between two  $Zn^{2+}$  ions to form a three-dimensional complex<sup>[25]</sup>. The grain size was increased as ammonia was added drop wise to the solution to adjust the pH below 7. A lower  $NH_3 \cdot H_2O / Zn(NO_3)_2$  molar ratio resulted in increased super saturation of the solution. Consequently, a great deal of ZnO precipitate was obtained from the solution by homogeneous nucleation in a short time, which inhibited the growth of the ZnO nanoparticles and led to a decrease in the ZnO grain size at a pH of 7. It was theorized that  $Zn^{2+}$  was stably complexed by ammonia for a high  $NH_3 \cdot H_2O / Zn(NO_3)_2$  molar ratio. As a result, heterogeneous nucleation of ZnO seldom occurred and the particles grew slowly<sup>[26]</sup> as shown in TABLE 1. The obtained ZnO nanoparticles were decorated on glass substrate and characterized by XRD spectra's is as shown in Figure 1B. A series of characteristic peaks are observed, and they are in accordance with the hexagonal wurtzite phase of ZnO crystalline peaks (JCPDS card no 89-139). No peaks of impurities were observed, suggesting that the high purity ZnO nanocrystalline film was obtained. In addition, the peak is widened little at pH =1 ZnO nanocrystalline film implying

that the particle size is small according to the Debye-Scherrer formula  $D = K / (\cos \theta)$  and the other characteristic peaks are still in accordance with the hexagonal wurtzite phase of ZnO films. The average crystallite size of the prepared different pH of ZnO nanocrystalline films as listed given in TABLE 2.

### Photo-physical properties

Figure 2 shows that the absorption spectra of the different grain sized ZnO nanocrystalline films shows the absorption peaks at 380, 374, 370 and 365 nm respectively for pH of 1,7,5 to pH of 3, which shows that by varying pH the wavelength shifts towards lower region. The optical properties are strongly dependent on the particle size i.e. blue shifted with respect to the bulk absorption edge appearing at 380nm<sup>[27]</sup>. It is clear that the absorption edge systematically shifts to the lower wavelength or higher energy with decreasing size of the nanocrystalline films. This pronounced and systematic shift in the absorption edge is due to the quantum size effect<sup>[28]</sup>. As known large particle showed a smaller surface area and void volume which influences a much higher light scattering ability than that of the small nanocrystalline films<sup>[29]</sup>. Hence, from the obtained absorbance the ZnO nanocrystalline films prepared at pH =3 and pH =5 are having high intensity then the absorbance spectra of ZnO nanocrystalline films prepared at pH =1 and pH =7 this is due to light scattering effect. Upon surface complex formation of heterocyclic azo sensitizer with different grain sized ZnO nanocrystalline films shifts the wavelength towards bathochromic

# ORIGINAL ARTICLE

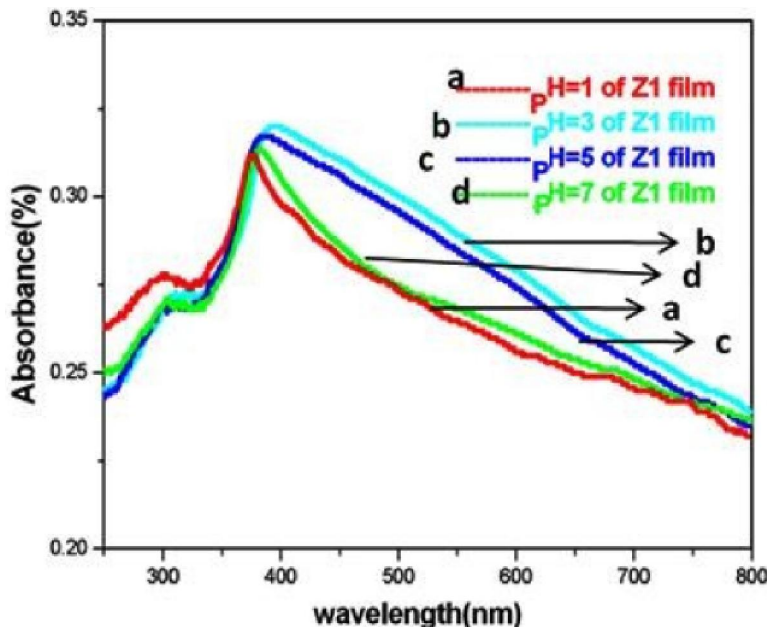


Figure 2 : UV-Visible absorbance spectra of different sized ZnO nanocrystalline films

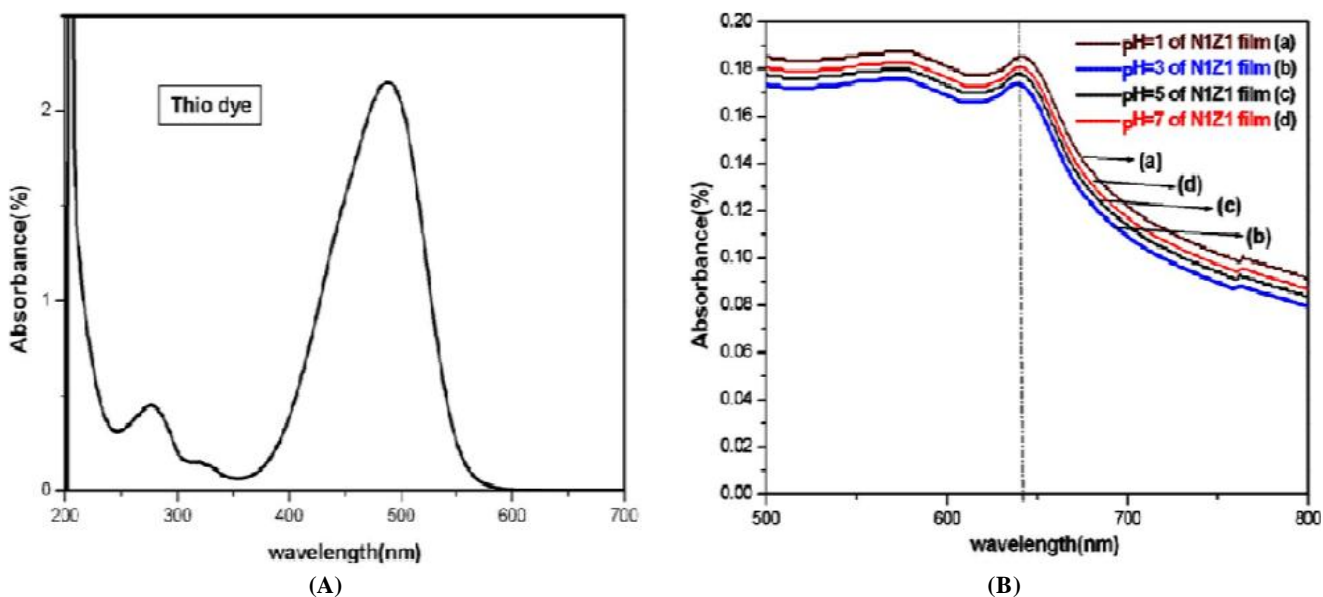


Figure 3 : [A] UV-Visible absorbance spectra of azo dye and [B] azo dye functionalized different sized ZnO nanocrystalline films

region, i.e. 430 to 630 nm corresponds to the electronic transition of the complex structure formed between ZnO nanocrystalline films and the dye structure. Also we examined that at different grain sized ZnO nanocrystalline films was dipped into the sensitizer solution which resulted has both bathochromic and hyperchromic shifts was observed at wavelength 630 nm<sup>[30]</sup>. This was attributed due to surface area of the ZnO nanocrystalline films and strong electronic interaction between the Zn (II) ions and non-

bonding electrons of nitrogen and deprotonation (-OH) of Phenolic group<sup>[31]</sup>.

## ATR-IR spectra of 3-[1, 3-benzothiazol-2-ylidiazanyl] naphthalen-2-ol sensitizer and N<sub>1</sub>-ZnO nanocrystalline film

The ATR-IR spectrum recorded for the N1 sensitizer chemisorbed ZnO surface gives a clear observation that interaction of dye structure with ZnO nanocrystalline as shown in Figure 4

The vibration bands at 1488.8 and 1528.5 cm-

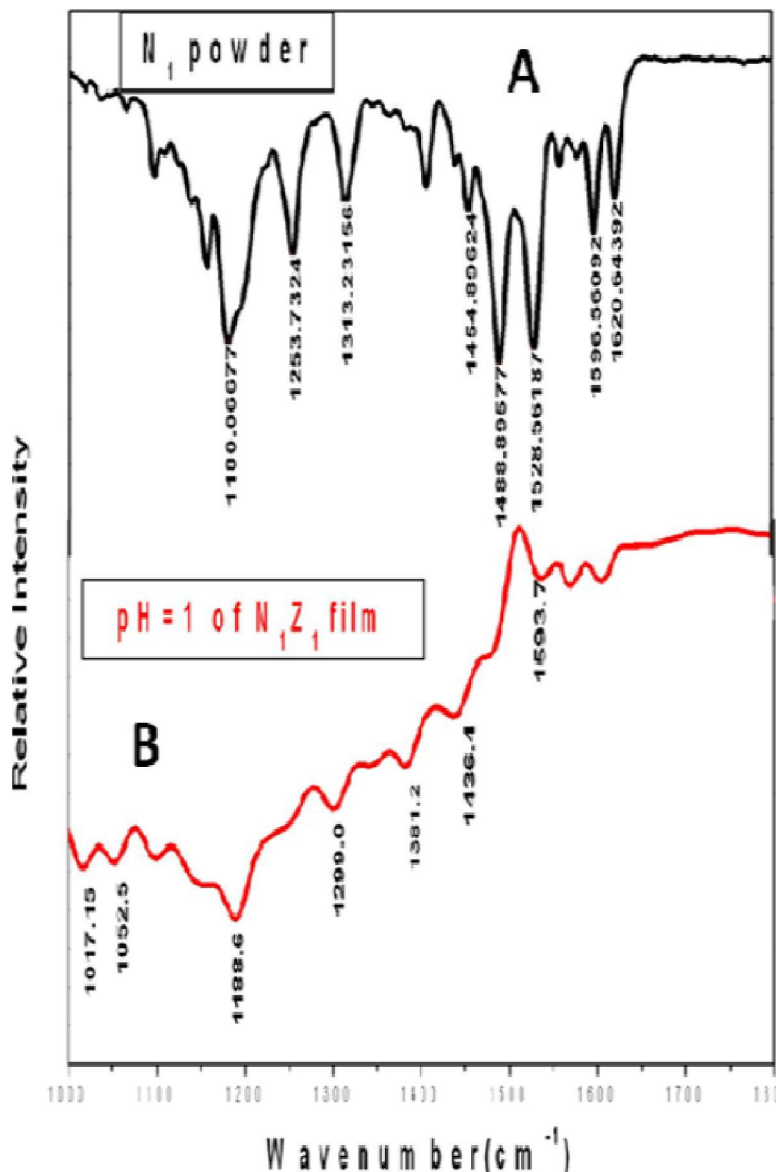


**Figure 4 :** ATR-IR spectral studies of [A] 3-[1, 3-benzothiazol-2-ylidiazonyl]naphthalen-2-ol dye (N<sub>1</sub>) and [B] N<sub>1</sub> sensitizer chemisorbed on ZnO nanocrystalline film

1 corresponds to N,N isomers of azo group and aromatic Phenolic group (-OH) stretching band at 1257  $\text{cm}^{-1}$  of azo sensitizer. The IR spectrum of N<sub>1</sub> sensitizer chemisorbed was little changed in the region 1250-1450  $\text{cm}^{-1}$ . The most prominent change was the band at 1257  $\text{cm}^{-1}$  (-OH of the Phenolic group) disappear or the Phenolic -OH group, on complexes shift with change in shape was observed indicating the engagement of this group in the coordination with the metal ion<sup>[31]</sup> and the band at 1436.4  $\text{cm}^{-1}$  was assigned to N=N stretching frequencies of dye-Zn complex. The results show that dinitrogen species have been greatly modified by coordination onto

Zn (II) ions i.e. N=N stretching frequency shifts towards lower region which states that engagement of this group to the central core of the Zn(II) ions.

### H<sup>1</sup>NMR of N<sub>1</sub> sensitizer

#### Antibacterial studies

By introducing immobilization of the photocatalyst several factors that influence the efficiency of the photocatalytic inactivation of microbes may be changed such as the access of light and oxygen to the photocatalyst surface, the distance between microbes and photocatalyst and possible penetration of the photocatalyst nanoparticles into microbe cells<sup>[32]</sup>.

# ORIGINAL ARTICLE

Although photoinactivation of bacteria should be more efficient in suspensions of a photocatalyst as compared to its immobilized form. The latter has a particular advantage as the immobilized photocatalyst may form a self-disinfecting and self-cleaning surface. Therefore, in our experiments the photoinactivation of bacteria was tested in the presence of immobilized visible light activated by functionalized ZnO films. Searching for surfaces easily self-disinfectable upon illumination with typical light sources as a result we decided to use a halogen lamp instead of a high pressure mercury lamp. The spectrum of the light emitted by a halogen lamp resembles the spectrum of diffuse daylight more than that emitted by a high pressure mercury lamp. It comprises only a very small part of UV-light necessary for direct excitation of unmodified ZnO film. These,  $N_1/ZnO$  sensitizer films whose photoactivation effect of *E. coli* bacteria were tested in the presence of visible light source. Apparently, under the experimental conditions immobilized form of the photocatalyst instead of suspension, significantly lower the photocatalytic activity because of the induced oxidative stress appeared to be insufficient for an effective bacteria inactivation.

The photo-assisted bactericidal effects of the dye-sensitized films on *E. coli* cells were tested under visible light source was filtered with a cutoff light

wavelength below 420 nm. The survival ratios of the bacterial cells in the system of ZnO nanocrystalline film and sensitizers under visible light irradiation does not change. These results indicate that pure ZnO nanocrystalline films alone or the dye alone has no apparent bactericidal activity under the corresponding experimental conditions as shown in Figure 6. To explore the optimum condition to achieve photo-inactivation of bacterial cells under visible irradiation will be the objective of the present work. The absorbance intensity and wavelength of the films is dependent on the generation of oxidative radicals for bactericidal inactivation. Similar observations have been reported Ying-Chan Hsu. et.al in the field of dye-sensitized solar cells showing that their energy conversion were dependent on the amount of dyes adsorbed and lack of absorption beyond  $>600$  nm<sup>[33]</sup>. Therefore at pH=1 of S1 sensitizer chemisorbed ZnO nano crystalline films shows higher photocatalytic activity as compared to the other pH level prepared ZnO nano crystalline films due to higher the surface area affects higher the chemisorption of sensitizers. From the Figure 6. Shows that N1Z1 films achieves the higher bactericidal effect than bare ZnO films. About 65-73 % of the *E. coli* cells were killed in 1 h as prepared with a different grain sized ZnO nano crystalline films (curve a-d) as shown in Figure 6. It is

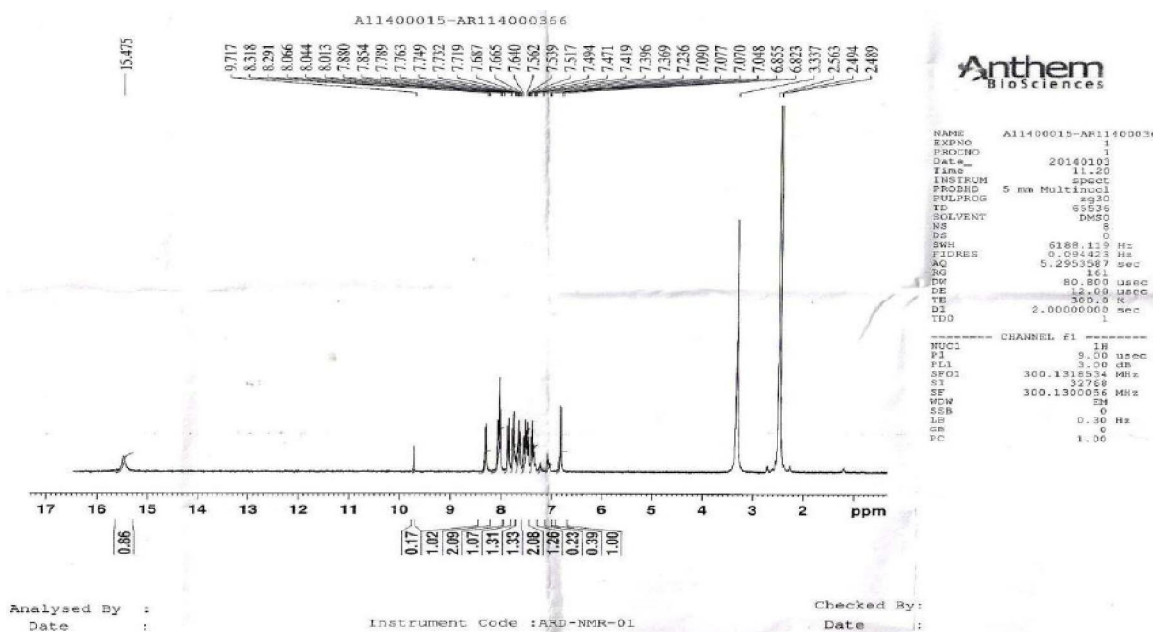
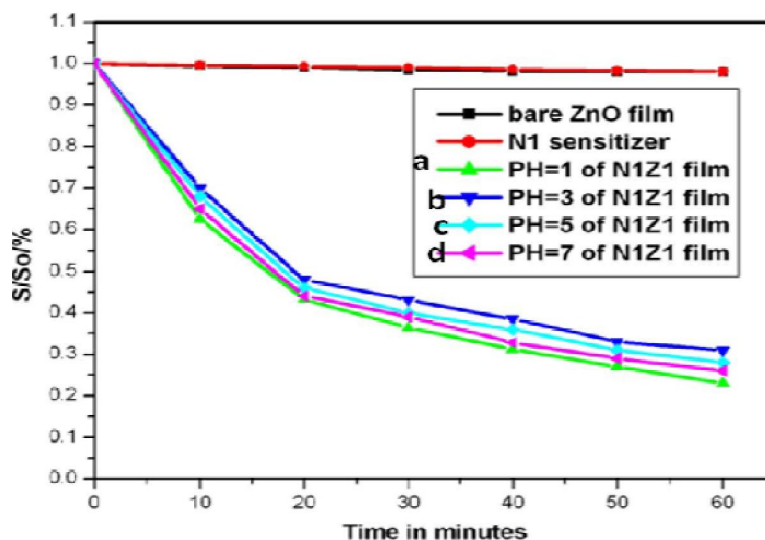


Figure 5 :  $^1H$  NMR N1 sensitizer



**Figure 6 : E-coli survival ratio of N1 sensitizers chemisorbed on different grain sized ZnO nano films under visible light irradiation**

because  $N_1Z_1$  films showing a absorption wavelength beyond  $>600$  nm, significantly the induced oxidative stress appeared to be sufficient for an effective bacteria inactivation, in the aerated aqueous solution, dissolved oxygen molecules accept an electron from the conduction band of ZnO and are transformed into superoxide anion radicals, which react with  $H_2O$  and generate other oxidative species such as hydrogen peroxide. The concentration of the oxidative species generated directly influences the killing rate for rate for E. coli cells.

## CONCLUSION

This paper presents the visible light induced photoactivity of functionalized zinc oxide crystalline films in the processes of E-coli bacteria killing. A significant effect of visible light illumination was observed in  $N_1$  sensitizer adsorbed zinc oxide crystalline films than bare zinc oxide crystalline films. The maximum photoinactivation requires relatively high visible light dosages, Hence  $N_1Z_1$  films achieves the higher bactericidal effect as compared with bare ZnO films. Particularly at pH = 1 prepared ZnO nanocrystalline films adsorbed with N1Z1 sensitizer showed a shift in the wavelength and absorbance Intensity towards higher region then the other pH levels (3,5,7) prepared ZnO nanocrystalline films due to the smaller the grain size is directly proportional to larger surface active sites which offers

higher the chemisorption of sensitizers on ZnO nanocrystalline films.

## REFERENCES

- [1] M.L.Curridal, R.Comparelli, P.D.Cozzli, G.Mascolo, A.Agostiano; *Mater.Sci.Eng.C.*, **23**, 285 (2003).
- [2] V.P.Kamat, R.Huehn, R.Nicolaescu, *J.Phys.Chem.B.*, **106**, 788 (2002).
- [3] Z.S.Wang, C.H.Huang, Y.Y.Huang, Y.J.Hou, P.H.Xie, B.W.Zhang, H.M.Cheng; *Chem.Mat.*, **13**, 678 (2001).
- [4] N.J.Cherepy, G.P.Smestad, M.Gratzel, J.Z.Zhang; *J.Phys.Chem.B.* 101, 9342 (1997).
- [5] A.Petrella, P.D.Cozzoli, M.L.Curri, M.Striccoli, P.Cosma, A.Agostiano; *Bioelectrochemistry*, **63**, 99 (2004).
- [6] A.Kay, M.Graetzel; *J.Phys.Chem.*, **23**, 6272 (1993).
- [7] S.Benjamin, D.Vaya, P.B.Punjabi, S.C.Ameta; *Arabian J.Chem.*, **4**, 205 (2011).
- [8] A.Zyoud; *Ph.D.Thesis*, An Najah National University, Palestine, 155 (2009).
- [9] A.Fujishima, K.Honda; *Nature.*, **238**, 37 (1972).
- [10] M.R.Hoffmann, S.T.Martin, W.Choi, D.W.Bahnamann; *Chem.Rev.*, **95**, 69 (1995).
- [11] J.C.Yu, J.Lin, D.Lo, S.K.Lam; *Langmuir*, **16**, 7304 (2000).
- [12] Z.Huang, P.C.Maness, D.M.Blake, E.J.Wolfrum, S.L.Smolinski, W.A.Jacoby; *J.Photochem.Photobiol.A.Chem.*, **130**, 163 (2000).
- [13] T.Matsunaga, M.Okuchi; *Environ.Sci.Technol.*, **29**, 501 (1995).

# ORIGINAL ARTICLE

---

- [14] Jing Liqiang, Wang Dejun, Wang Baiqia, Li Shudan, Xin Baifu, Fu Honggang, Sun Jiazhong; *J.molecular Catalysis.A*, **244**, 193 (2006).
- [15] A.Hagfeldt, M.Gratzel; *Chem.Rev.*, **95**, 49 (1995).
- [16] F.Lenzmann, J.Krueger, S.Burnside, K.Brooks, M.Gratzel, D.Gal, S.Ruhle, D.Cahen; *J.Phys.Chem.B.*, **105**, 6347 (2001).
- [17] M.K.Nazeeruddin, P.Pechy, T.Renouard, S.M.Zakeeruddin, R.Humphry Baker, P.Comte, P.Liska, L.Cevey, E.Costa, V.Shklover, L Spiccia, G.B.Deacon, C.A.Bignozzi, M.Gratzel; *J.Am.Chem.Soc.*, **123**, 1613 (2001).
- [18] S.A.Haque, Y.Tachibana, R.L.Willis, J.E.Moser, M.Gratzel, D.R.Klug, J.R.Durrant; *J.Phys.Chem.B.*, **104**, 538 (2000).
- [19] U.Bach, D.Lupo, P.Comte, J.E.Moser, F.Weissortel, J.Salbeck, H.Spreitzer, M.Gratzel; *Nature*, **395**, 583 (1998).
- [20] Y.M.Cho, W.Y.Choi, C.H.Lee, T.Hyeon, H.I.Lee; *Environ.Sci.Technol.*, **35**, 966 (2001).
- [21] Sondos Othman Abed Alhadi Ateeq; *Thesis*, 1 (2012).
- [22] H.Vijay patel, P.Manish patel, G.Ranjan patel; *J.Serb.Chem.Soc.*, **67**, 727 (2002).
- [23] C.T.Keerthi kumar, J.Keshavayya, T.Rajesh, Peethamba; *Int.J.Pharm.Pharm.Sci.*, **5**, 296 (2013).
- [24] Y.L.Zhang, Y.Yang, J.H.Zhao, R.Q.Tan, P.Cui, W.J.Song; *J Sol-Gel Sci Technol.*, **51**, 198 (2009).
- [25] A.Hardy, J.D.Haen, M.K.Van Bael, J.Mullens; *J Sol-Gel Sci Technol.*, **44**, 65 (2007).
- [26] K.Yu, Z.G.Jin, X.X Liu, Z.F Liu, Y.N Fu; *Mater Lett.*, **61**, 2775 (2007).
- [27] P.Virendra, D.Charlnene, Y.Deepti, A.J.Shaikh, V.Nadanathangam; *Spectrochemica Acta part A.*, **65**, 173 (2006).
- [28] M.Soosen Samuel, Lekshmi Bose, K.C.George; *Acedamic Review*, **1**, 57 (2009).
- [29] B.Munkhbayar, M.Dorjderem, D.Sarangerel, Bayanjargal Ochirkhuyag; *Nanosci.Nanotechnol.Lett*, **5**, 1 (2013).
- [30] D.EL.Mekkawi, M.S.A.Abdel Mottaleb; *International Journal of Photo energy*, **7**, 95 (2005).
- [31] Heather Gulley, Stahl, Patricka, Hoganii, Whitney, Schmidt, Staphen J.Wall, Andrew uhrlage, Heather; *Bullen Environ.Sci.Technol.*, **44**, 4116 (2005).
- [32] C.Srinivasan, N.Somasundaram; *Curr.Sci.*, **85**, 25 (2003).
- [33] Ying Chan Hsu, Hegen Zheng, Jiann T'suen Lin, Kuo-Chuan Hoa; *Solar Energy Materials & Solar Cells*, **87**, 357 (2005).